SERBIAN JOURNAL OF ELECTRICAL ENGINEERING
Vol. 23, No. 3, October 2026, 353-375
UDC: 621.313.12: 517.443 **DOI: https://doi.org/10.2298/SJEE2603353D**
Original scientific paper

Time-domain Modelling of Low-power Transformer for Power Supply Applications

Srđan Divac[1], Krzysztof Chwastek[2], Mariusz Najgebauer[2], Branko Koprivica[1]

Abstract: The aim of this paper is to present a way of solving an electrical circuit of a single-phase transformer with a nonlinear hysteretic core in the time domain. The considered circuit consists of an AC power supply, a transformer with a ring-shaped core and a resistor in the transformer primary and secondary circuit depicting the coil ohmic resistances. The secondary circuit also has a load impedance. Three working regimes of the transformer are considered – when it is loaded and when it is close to no-load and short-circuit working conditions. For the loaded regime, impedance has been varied from 10 Ω to 10 kΩ, with power factor from 0.01 to 0.99. In the no-load and short circuit regimes it is set to 10 MΩ and 0.01 Ω, respectively, with the power factor of 0.99. Calculations have been made at industrial frequency (50 Hz) using an iterative procedure based on Harmonic Interpolation Method (HIM) and Bertotti's Statistical Theory of Losses (STL). The obtained results are compared with the results calculated using an equivalent transformer circuit and well-known *RL* model of the transformer core. The details regarding the calculation procedures, measurement setup and results, the comparison of the calculated results, as well as their appropriate analysis, are presented in this paper.

Keywords: Single-phase transformer, Ring-shaped core, Harmonic Interpolation Method, RL model, Time domain.

1 Introduction

Transformers are part of modern power engineering systems and have a significant effect on their efficiency. Therefore, accurate solving of electric

[1]University of Kragujevac, Faculty of Technical Sciences Čačak, Serbia
srdjan.divac@ftn.kg.ac.rs, https://orcid.org/0000-0002-7093-9529
branko.koprivica@ftn.kg.ac.rs, https://orcid.org/0000-0001-5014-6866
[2]Czestochowa University of Technology, Faculty of Electrical Engineering, Częstochowa, Poland
krzysztof.chwastek@pcz.pl, https://orcid.org/0000-0002-2294-9976
mariusz.najgebauer@pcz.pl, https://orcid.org/0000-0001-9441-1924
*An earlier version of this paper was presented at the 13th International Conference on Electrical, Electronic and Computing Engineering (IcETRAN), Silver Lake, Serbia, June 2026.

© *Creative Common License CC BY-NC-ND*

circuits with a transformer in the time domain is of great importance. However, the nonlinear hysteretic properties of electrical steel sheets used to make laminated cores often make the calculations more challenging. This is mainly due to the appearance of higher harmonics in the magnetic field strength $H(t)$ and/or magnetic flux density $B(t)$ waveforms caused by the nonlinearity of the core material [1]. The performance of the core may be assessed either from an appropriate analytical description of hysteresis, RL circuit model or with some other method [2 – 8].

The use of hysteresis models generally offers the most accurate solution in the time domain, but identification of their parameters can be time-consuming. At the same time, mathematical complexity of the models can greatly limit their practical application [9]. An iterative procedure for solving a dynamic electric circuit with nonlinear hysteretic inductor in time domain has been proposed in previous publications [10, 11]. It combines a novel Harmonic Interpolation Method (HIM) and Bertotti's Statistical Theory of Losses (STL). It is aimed at taking into account the influence of hysteresis phenomena without the use of complicated hysteresis models [12]. This procedure has been incorporated into the procedure for solving an electric circuit with single-phase transformer with ring-shaped core [13]. However, only purely ohmic loads have been considered, therefore a general perspective into the capabilities of the proposed procedure has not been assessed properly. This paper considers a similar electric circuit but with a more realistic linear load.

The considered electric circuit consists of AC power supply, single-phase transformer with ring-shaped core, two resistors connected in series with the primary and secondary transformer coils and a load impedance. Solutions have been found for three working regimes of the transformer – when it is loaded and when it is close to the no-load and short-circuit working conditions. For loaded regime the impedance has been varied from 10 Ω to 10 kΩ, with power factor from 0.01 to 0.99. In the no-load and short circuit regimes it is set to 10 MΩ and 0.01 Ω, respectively, with the power factor of 0.99.

Time domain calculations have been performed for sinusoidal input voltage amplitudes from 30 V to 120 V with the step of 30 V. Its frequency has been set to the industrial frequency of 50 Hz, as is common in power engineering. Results obtained with the proposed iterative procedure have been compared to the ones obtained using parallel *RL* model. The parameters necessary for the implementation of the considered approaches have been obtained from measurement results. Measurements have been made with a ring-shaped sample of electrical steel while controlling the shape of $B(t)$ waveform. The shape of controlled waveform has been set to sinusoidal with amplitudes $B_{\max}$ from 0.2 T to 1.6 T, with measurement step of 0.2 T, at quasistatic and dynamic frequencies of 1 Hz and 50 Hz, respectively.

The details regarding the two approaches (iterative procedure and *RL* model), measurement and calculation results, comparison of waveform shapes, differences in effective values and calculated transformer energy efficiency, as well as their appropriate analysis are presented.

2 Calculation Approach

An electrical circuit with a single-phase transformer having a ring-shaped core has been considered. Transformer primary coil, with N_1 turns, has been connected in series with a resistor R_{N1} and AC power source $u(t)$. The load of the transformer has been modeled using an impedance Z with the power factor of cosφ and connected to the resistor R_{N2} and transformer secondary coil with N_2 turns. The resistors R_{N1} and R_{N2} represent the ohmic resistance of primary and secondary transformer coils, respectively. Magnetic flux leakage has been neglected for both coils. The considered electrical circuit is presented in Fig. 1.

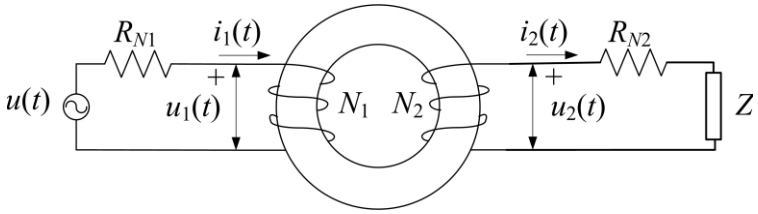


Fig. 1 – *Considered electrical circuit with a single-phase transformer.*

Two approaches have been considered when solving the aforementioned circuit – first, through an iterative procedure using HIM and STL and second, using *RL* model.

2.1 Iterative procedure

The first approach is an application of the iterative calculation procedure, previously applied to solve an electrical circuit with a nonlinear hysteretic inductor in time domain [11]. The core of the procedure is the HIM methodology which can be used to accurately simulate hysteretic behavior of the electrical steel. This is done by means of the harmonic analysis of measurement data and interpolation of the obtained amplitudes and phases of the harmonics. It is, however limited by the frequency and shape of the waveforms controlled during the measurements, which can be mitigated by expanding it according to STL.

The iterative procedure can be carried out through the following steps:

1. Calculation of voltage at the transformer primary coil $u_{1,j}(t)$, using Kirchhoff law:

$$u_{1,j}(t) = u(t) - R_{N_1} i_{1,j-1}(t), \tag{1}$$

where j is the order of the current iteration. For initial condition, it has been deemed sufficient to choose $i_{1,0}(t)=0$, for every instance of time t;

2. Calculation of core magnetic flux density $B_{c,j}(t)$, using Faraday law:

$$B_{c,j}(t)=\frac{1}{N_1 S_c}\int_o^t u_{1,j}(\tau)\,\mathrm{d}\tau, \tag{2}$$

where S_c is the cross-sectional area of the ring-shaped transformer core;

3. Calculation of the cores magnetic field strength $H_{c,j}(t)$, corresponding to the $B_{c,j}(t)$, using a combination of HIM and STL methodology. According to STL, $H_{c,j}(t)$ can be separated into its three components – quasistatic $H_{qs,j}(t)$, eddy current $H_{eddy,j}(t)$ and excess $H_{exc,j}(t)$ magnetic field component [12]. First component, $H_{qs,j}(t)$, is obtained by first simulating quasistatic $H(t)$ for the amplitude of $B_{c,j}(t)$, $B_{\max,j}$, using HIM and measurements at low frequency under controlled sinusoidal $B(t)$ waveform shape. The newly found $H(t)$ corresponds to the shape of controlled $B(t)$, not $B_{c,j}(t)$. However, the shape of the quasistatic hysteresis loop, formed from obtained $H(t)$ and $B(t)$ corresponding to the shape of controlled $B(t)$ waveform, will remain the same for both $B(t)$ and $B_{c,j}(t)$ [14]. As such, its necessary to form the aforementioned quasistatic hysteresis loop and then reconstruct it for the $B_{c,j}(t)$ waveform. Second and third components of $H_{c,j}(t)$ are calculated using well-known expressions [12]:

$$H_{eddy,j}(t)=\frac{\sigma d^2}{12}\frac{\mathrm{d}B_{c,j}(t)}{\mathrm{d}t}, \tag{3}$$

$$H_{exc,j}(t)=\frac{n_0 V_0}{2}\left(\sqrt{1+\frac{4\sigma G S_c}{{n_0}^2 V_0}\frac{\mathrm{d}B_{c,j}(t)}{\mathrm{d}t}}-1\right), \tag{4}$$

where d is the core electrical steel sheet thickness, σ is its electrical conductivity, n_0 and V_0 are the phenomenological parameter and G is equal to 0.1356. Phenomenological parameters can be obtained from quasistatic and dynamic measurements following the procedure first proposed by Bertotti [15]. Finally, $H_{c,j}(t)$ is calculated from (5):

$$H_{c,j}(t)=H_{qs,j}(t)+H_{eddy,j}(t)+H_{exc,j}(t); \tag{5}$$

4. Calculation of voltage at the transformers secondary coil $u_{2,j}(t)$, using (6):

$$u_{2,j}(t)=N_2 S_c\frac{\mathrm{d}B_{c,j}(t)}{\mathrm{d}t}; \tag{6}$$

5. Calculation of the secondary current $i_{2,j}(t)$ by solving the differential equation with linear parameters (7):

$$u_{2,j}(t) - \left(R_{N_2} + R\right) i_{2,j}(t) - L\frac{\mathrm{d}i_{2,j}(t)}{\mathrm{d}t} = 0, \tag{7}$$

where R and L are the ohmic resistance and inductance of the load, calculated from (8) and (9):

$$R = Z\cos\varphi, \tag{8}$$

$$L = \frac{Z\sin\varphi}{2\pi f}, \tag{9}$$

where f is the frequency of $u(t)$.

In general, the voltage waveform $u_{2,j}(t)$ can be non-sinusoidal, so it is recommended to solve (7) numerically in time domain;

6. Calculation of temporary solution for primary current, $i_1{}'_{,j}(t)$:

$$i_1{}'_{,j}(t) = \frac{H_{c,j}(t) l_c + N_2 i_{2,j}(t)}{N_1}, \tag{10}$$

where l_c is the magnetic path length of the ring-shaped core;

7. Calculation of primary current, $i_{1,j}(t)$:

$$i_{1,j}(t) = \frac{i_i{}'_{,j}(t) + i_{i,j-1}(t)}{2}. \tag{11}$$

This step slows down the iterative procedure, therefore allowing one a more stable convergence of the results;

8. Checking if the criterion for the convergence of $i_{1,j}(t)$, ε, is met. The criterion for the convergence has been chosen as:

$$\frac{\max\left\{\left|i_{1,j}(t) - i_{1,j-1}(t)\right|\right\}}{\max\left\{\left|i_{1,j}(t)\right|\right\}} 100 \le \varepsilon. \tag{12}$$

It can be very strict due to step 7). In case when (12) is not true, the steps 1 – 7 need to be repeated, but when it is, the iterative procedure ends.

2.2 RL model

The second approach to solving the circuit in Fig. 1 uses an equivalent transformer circuit with parallel *RL* model approach to represent its nonlinear hysteretic core [16]. The resistor R_c represents the power loss of the transformer core and has been chosen as linear and its value calculated using the measurement results for the major hysteresis loop and (13) – (15). The use of major hysteresis loop in the calculation has been chosen since it is commonly provided by the manufacturers.

$$R_c = \frac{U^2}{P_c}, \tag{13}$$

$$U = N_1 S_c \sqrt{\frac{1}{T}\int_0^T \left(\frac{\mathrm{d}B}{\mathrm{d}t}\right)^2 \mathrm{d}t}, \tag{14}$$

$$P_c = \frac{S_c l_c}{T}\int_0^T H(t)\frac{\mathrm{d}B(t)}{\mathrm{d}t}\mathrm{d}t, \tag{15}$$

where $T = 1/f$.

The inductor L_c represents the nonlinearity of the core and has been characterised as nonlinear, using a measured piece-wise magnetisation curve (B-H curve). This is one of the commonly used approaches as Rezaei-Zare commented upon in his research [7]. The ideal transformer equivalent circuit with the transformation ratio of N_1:N_2 has been used to couple the primary and secondary transformer circuits. The load with the impedance Z and power factor cosφ is modelled as a linear resistor R and inductor L connected in series and calculated using (7) and (8). The equivalent electrical circuit according to this approach, with the load represented as Z, is shown in Fig. 2.

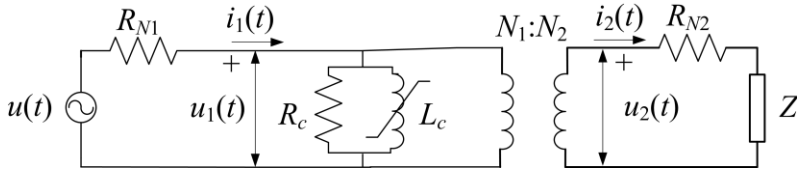


Fig. 2 – *Considered electrical circuit implementing the RL model of the core.*

3 Measurements

Magnetic field strength $H(t)$ and magnetic flux density $B(t)$ waveforms have been measured indirectly, using measurement setup incorporating data acquisition system and PC [17]. The details regarding setup components, measurement procedure, as well as the principle of B(t) waveform control realised using a software-based feedback loop, can be found in a recent PhD thesis [18].

The basis of HIM is the harmonic analysis of the measurement results. As such, its accuracy is directly influenced by the quality of the of the measurements. Measurements have been made using a ring-shaped sample. Core of the sample has been formed by winding a sheet of 27PH100 electrical steel with thickness d, width w and electrical conductivity σ. The sheet has been manufactured by POSCO and is usually used for forming laminated transformer cores [19]. Based on the inner r_i and outer r_o radius of the core, magnetic path length of the ring core is $l_{cS}=(r_i+ r_o)\pi$. Over the core, two coils have been wound - primary coil of

N_1 turns with the resistance of R_{N1}, and secondary coil of N_2 turns with the resistance of R_{N2}, using copper wire of the same cross-sectional area. Parameters of the ring-shaped sample are shown in **Table 1**.

Table 1
Parameters of the ring-shaped sample.

Parameter	Value	Parameter	Value
N_1	175	R_{N_1} [Ω]	0.8
N_2	61	R_{N_2} [Ω]	0.27
r_i [mm]	45	r_o [mm]	52.5
l_{cS} [m]	0.306	S_{cS} [mm2]	102.80
d [mm]	0.27	σ [kS/m]	2083
w [mm]	15	-	-

Two sets of measurements have been made, one at frequency of 50 Hz, while the other at a low frequency of 1Hz. This frequency has been deemed low enough so that the dynamic effects are negligible, compared to the ones at 50 Hz, and thus the excitation conditions can be regarded as quasistatic [2, 14]. Both sets have been made for controlled $B(t)$ waveform with sinusoidal shape and amplitudes $B_{\max}$ from 0.2 T to 1.6 T, with measurement step of 0.2 T. Measurement results for both dynamic and quasistatic measurements are presented in the form of hysteresis loops in Figs. 3 and 4, respectively. Measured piece-wise magnetisation (B-H) curve at 50 Hz has been obtained by linearly connecting the amplitudes of measured $H(t)$ and $B(t)$ and is also shown in Fig. 3. All measurements have been made for 1000 data points.

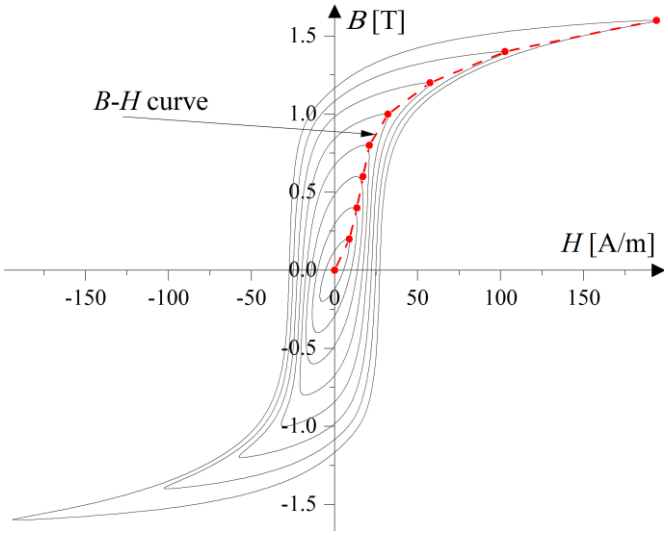


Fig. 3 – *Measured hysteresis loops and B-H curve at* 50 Hz.

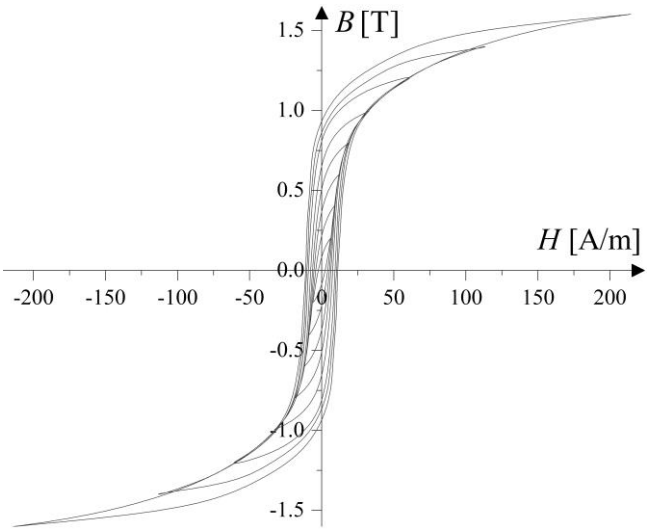


Fig. 4 – *Measured hysteresis loops at* 1 Hz.

4 Results and analysis

The targeted nominal voltage transformation ratio of the considered transformer U_n/U_{sn} is 70/24 V/V and a relatively low apparent power of about 30 VA under nominal working conditions. Similar transformers are used for powering electronic devices and designing stable linear DC power sources and small chargers. This is because such AC voltage, when rectified and filtered accordingly, could provide about 30 V DC at no-load. Parameters of the transformer ring-shaped core of 27PH100 electrical steel and primary and secondary coil are shown in **Table 2**.

Table 2
Parameters of the considered transformer ring-shaped core.

Parameter	Value	Parameter	Value
N_1	350	R_{N_1} [Ω]	3.95
N_2	120	R_{N_2} [Ω]	1.33
r_i [mm]	83.6	r_o [mm]	111.4
l_{cS} [m]	0.612	S_{cS} [mm2]	771
d [mm]	0.27	σ [kS/m]	2083
w [mm]	27.76	-	-

Calculations have been made for three working regimes of the transformer in Fig. 1 – no-load, loaded and short-circuit. First and third are considered by setting Z to 10 MΩ and 0.01 Ω, respectively, with the cosφ of 0.99. The

calculations for the loaded conditions have been made for Z of 10, 100, 1000 and 10000 Ω, with the power factor from 0.01 to 0.99. This allows one the analysis of not only the effect of the load current amplitude for loads significantly different than the nominal one, but also its phase shift on the overall calculation procedure.

Input voltage has been chosen as sinusoidal with amplitude U_m from 30 V to 120 V, with the step of 30 V, and industrial frequency of 50 Hz. The upper voltage limit considers the case of overvoltage of about 20% of the transformer primary nominal voltage value, guaranteeing higher level of saturation of the ring core than in the case of transformer nominal working conditions. The chosen voltage range ensures that cases of core behaviour of close to linear and distinctly nonlinear, as well as the cases in-between, have been taken into account, therefore ensuring the objectiveness of this research.

Time domain calculations based on the proposed iterative procedure (first approach) have been made using Wolfram Mathematica software, with 1000 calculation points. Differential equation (7) has been solved numerically, using *DSolve* built-in function. To make sure that only the steady-state solution is used, first 500 periods of the resulting load current waveform have been neglected.

HIM methodology parameters for local spline interpolation – amplitudes and phases interpolation orders (n_a and n_p) and total number of odd harmonics of interest i, have been set to n_a=3, n_p=1 and N=6. These parameters are influenced by measured $H(t)$ and $B(t)$ waveforms for 27PH100 electrical steel so they have been taken from previous research with identical core material and measurement conditions [11]. However, the proposed n_0 and V_0 parameters could not be reused since only the frequency of 50 Hz has been taken into account in this paper. The transformer core is also significantly larger than the core of the inductor considered in the aforementioned research. As such, these parameters have been recalculated following the proposed procedure using measured dynamic and quasistatic hysteresis loops and core parameters from **Table 2**. It has been found that the best fit for values of interest can be achieved for the pair of n_0=3079 and V_0= 0.0025 A/m.

The convergence criterion, ε, has been keep at constant value of 0.01% for all calculations.

A model has been made using MATLAB Simulink and its *Simscape* library to solve the equivalent circuit from Fig. 2 (second approach). The model is shown in Fig. 5. Simulations have been made using Backward Euler solver and fixed simulations step of 20 μs (1000 calculation points per period T). However, the results have been presented with fewer data points. This is to achieve better visualisation of the results and has no effect on their accuracy.

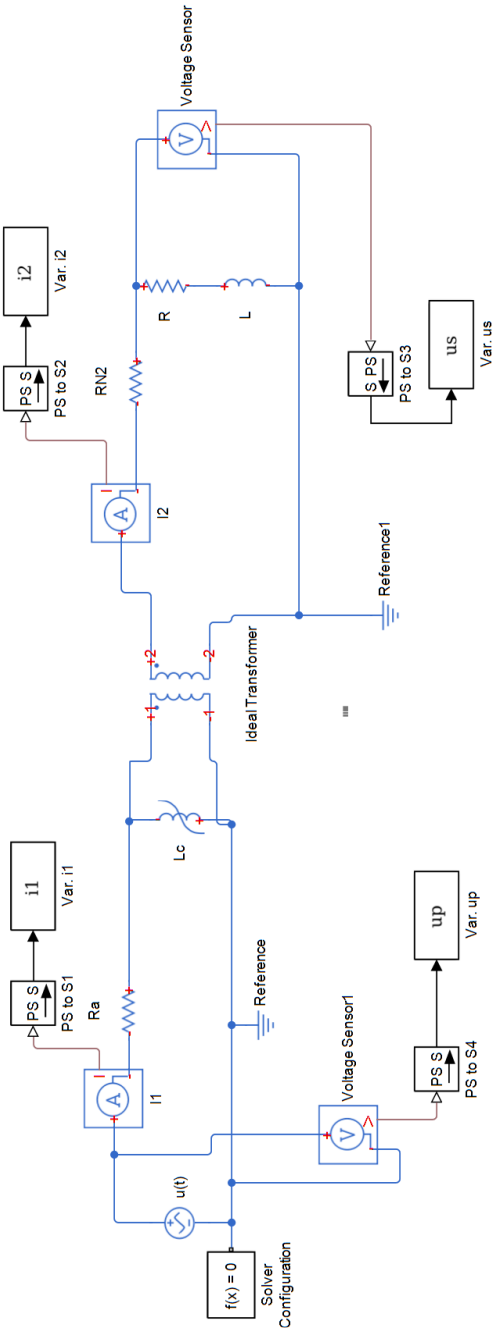


Fig. 5 – *MATLAB Simulink model.*

Parallel *RL* circuit from Fig. 2 has been exchanged with nonlinear inductor model which takes into account R_c as linear and L_c as nonlinear element, connected in parallel. These parameters have been calculated from measurements at 50 Hz and parameters from **Table 2** – $R_c = 2149$ Ω using (13) – (15) and waveforms at 1.6 T (considered as main hysteresis loop measurements), and L_c by forming *B-H* magnetisation curve presented as dashed line in Fig. 3.

In Figs. 6 – 11 the comparison of the results for $i_1(t)$ obtained using two considered approaches, for all considered *Z* and power factor of 0.99, is shown.

The waveforms in Fig. 6 have distorted shapes, The distortion increases with the increase in U_m. This is because in no-load working condition the influence of the secondary current on the primary one is negligibly small due to the low power requirements of the load. As such, most of the supplied power is used for the magnetisation of the transformer core and not transferred to the load. The results in Fig. 6 are very similar to the ones in Figs. 7 and 8 for all corresponding U_m. However, the numerical analysis is necessity to determine if the difference in the displayed corresponding waveforms are low enough to indicate that the case of *Z*=1 kΩ can be considered as no-load condition for the considered transformer.

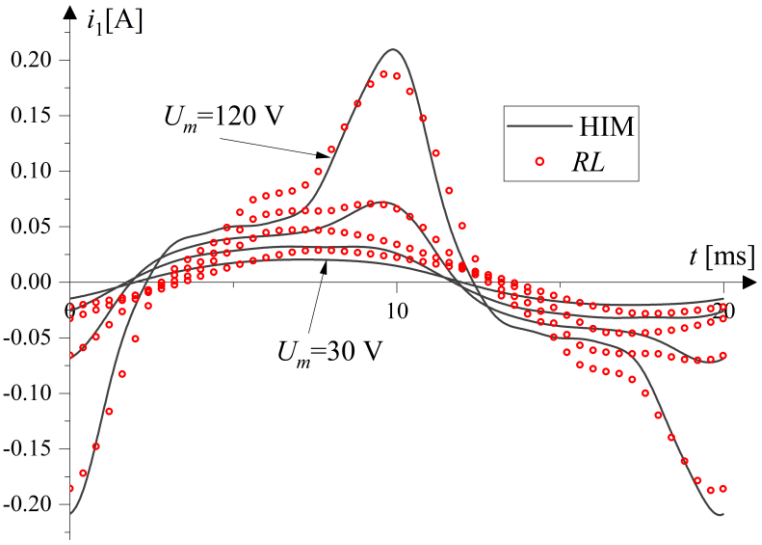


Fig. 6 – *Comparison of $i_1(t)$ obtained using HIM and RL model for Z=* 10 MΩ *and* $\cos\varphi$=0.99, *Um from* 30 V *to* 120 V *with the step of 30 V, at* 50 Hz.

Calculation results for iterative procedure made when considering the electrical circuit with nonlinear hysteretic inductor at 50 Hz show a very good agreement with the measurements [11]. As the considered electrical circuit is quite similar to the one considered in this paper when the transformer performs very close to the no-load working condition – *Z*=10 MΩ, the aforementioned

results suggest that the results in Fig. 6, and by extent Figs. 7 – 10, show better agreement with measurements when obtained using HIM than with *RL* model.

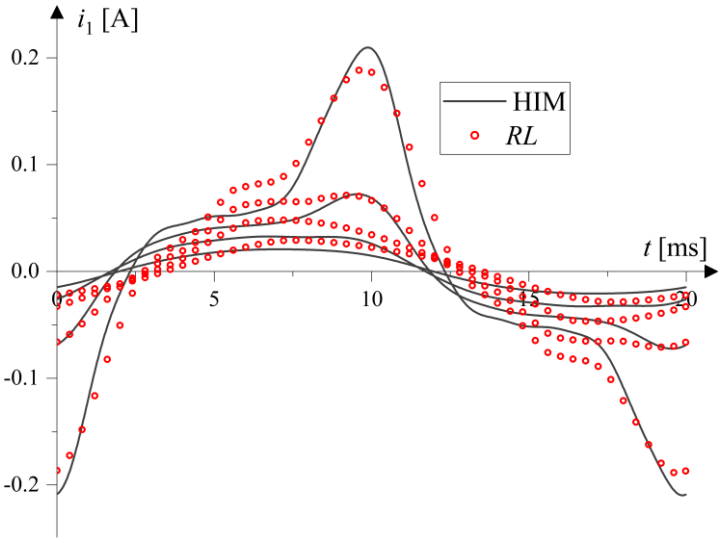


Fig. 7 – *Comparison of $i_1(t)$ obtained using HIM and RL model for Z*= 10 kΩ *and* cos*φ*=0.99*, Um from* 30 V *to* 120 V *with the step of* 30 V*, at* 50 Hz*.*

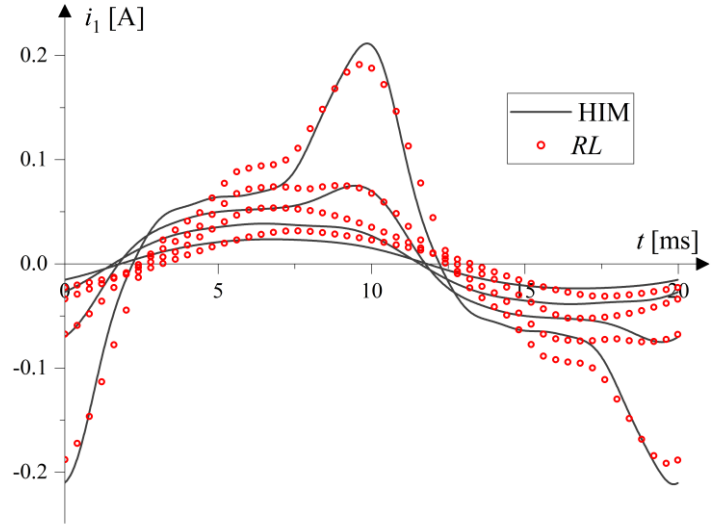


Fig. 8 – *Comparison of $i_1(t)$ obtained using HIM and RL model for Z*= 1 kΩ *and* cos*φ*=0.99*, Um from* 30 V *to* 120 V *with the step of* 30 V*, at* 50 Hz*.*

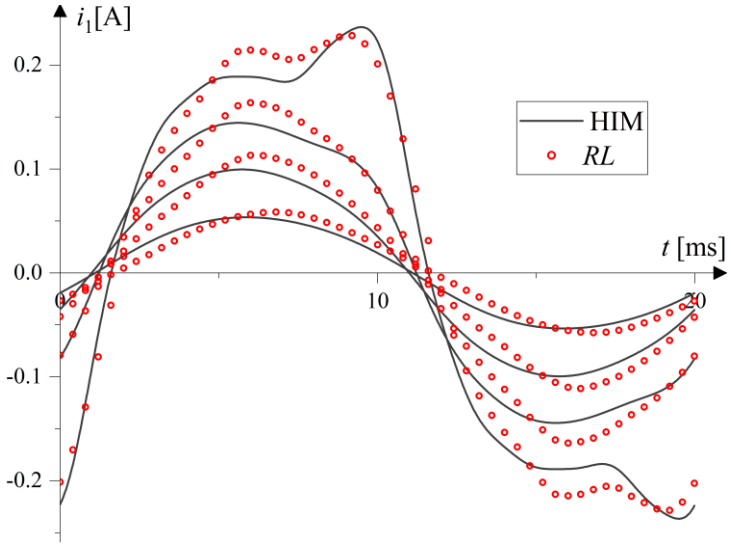


Fig. 9 – *Comparison of $i_1(t)$ obtained using HIM and RL model for Z=100 Ω and cosφ=0.99, Um from* 30 V *to* 120 V *with the step of* 30 V, *at* 50 Hz.

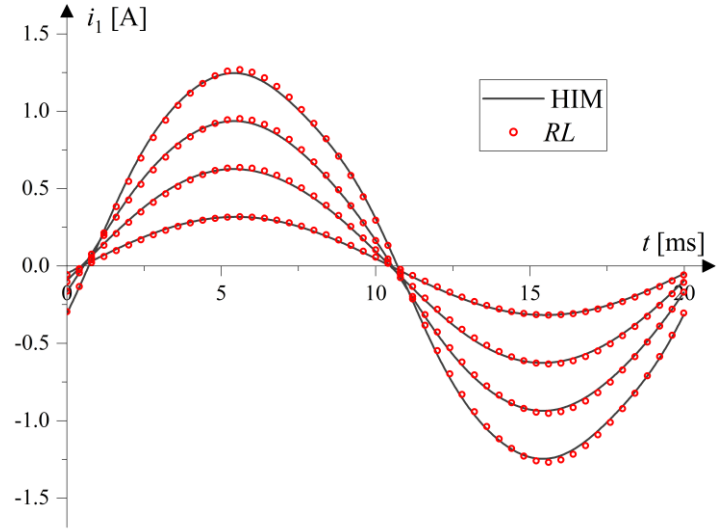


Fig. 10 – *Comparison of $i_1(t)$ obtained using HIM and RL model for Z=10 Ω and cosφ=0.99, Um from* 30 V *to* 120 V *with the step of* 30 V, *at* 50 Hz.

Comparisons of the results presented in Figs. 6 – 10 show significant differences in amplitude and phase shift for the two considered approaches. It can be noted that in most cases of U_m, the results exhibit overall higher amplitudes

when obtained with *RL* modelling approach than when using HIM, exception being in cases of increased nonlinearity, such as for U_m of 120 V. Additionally, in some cases such as the case for of 90 V in Figs. 6 – 8 and 120 V in Fig. 9, HIM methodology offers less oscillatory solution than the one using *RL* model.

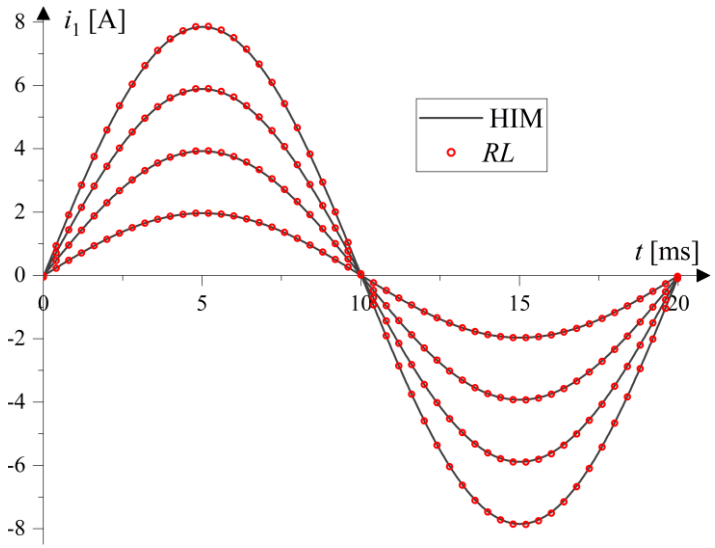


Fig. 11 – *Comparison of $i_1(t)$ obtained using HIM and RL model for Z*=0.01 Ω *and* cosφ=0.99*, Um from* 30 V *to* 120 V *with the step of* 30 V*, at* 50 Hz*.*

Decreasing of the impedance Z increases the influence of the secondary current on the primary one, as can be seen from Figs. 8 – 11. When the impedance reaches the value of 10 Ω (Fig. 10), the waveforms of $i_1(t)$ obtained for the two approaches are very similar and close to being sinusoidal in shape. This is due to the fact that the highest contribution to the $i_1(t)$ is of the secondary current, not the one used to magnetise the core – point of interest for the two approaches. This is further proven by comparing the amplitudes of the waveforms in Figs. 6 and 10, which shows that the one in Fig. 10 obtained for 120 V, is almost 6 times higher than the one in Fig. 6 for no-load conditions - when the influence of the magnetising current is the most prominent. Secondary current is very close to sinusoidal as the voltage drop over R_{N1}, and R_{N2} is low enough not to significantly influence the shape of the secondary voltage waveform, compared to the primary one. However, the waveforms in Fig. 10 are not identical for both approaches. Higher amplitude can be observed for the for the calculations made using *RL* model. This means that, even though the influence of the secondary current is significant, its still not enough to fully compensate for the different calculation approaches to modelling of the transformer core.

The difference in the approaches does not affect the calculations for the short-circuit working regime, as can be seen in Fig. 11. The waveforms are sinusoidal in shape and are in a very good agreement for both considered approaches. This is because the influence of the secondary sinusoidal current is significantly higher than in all of the previous cases, which can be proven by the amplitude of the primary current being more than 35 times higher than the one during the no-load calculations for the same U_m.

Further analysis can be made by comparing the effective values of $i_1(t)$, I_1, for both approaches with respect to Z, cosφ and U_m. Relative difference δI_1 is calculated using (16) and is shown in **Table 3**. The comparison of the results for short-circuit and no-load regime have only been made for cosφ=0.99.

$$\delta I_1 [\%] = \frac{\sqrt{\frac{1}{T}\int_0^T \left(i_{1,RL}(t)\right)^2 \mathrm{d}t} - \sqrt{\frac{1}{T}\int_0^T \left(i_{1,\mathrm{HIM}}(t)\right)^2 \mathrm{d}t}}{\sqrt{\frac{1}{T}\int_0^T \left(i_{1,\mathrm{HIM}}(t)\right)^2 \mathrm{d}t}} 100, \tag{16}$$

where $i_{1,\mathrm{HIM}}(t)$ and $i_{1,RL}(t)$ are results for $i_1(t)$ obtained using iterative procedure and *RL* model, respectively.

Most of the results in **Table 3** are positive, suggesting that the approach using the iterative procedure gives lower I1 than the approach based on *RL* model, the exception being -0.02%. Reason most likely being the error in numerical calculations. This can be of interest when designing hazard mitigation equipment for the transformers.

Differences of less than 0.35% can be noted in the case of 0.01 Ω and power factor of 0.99. This confirms that the results in short-circuit regime are in very good agreement for both approaches. Its interesting to note that the rate of change of δI_1 as Z increases slows down significantly for values over 10 kΩ, even though the Z increases 1000 times, compared to other considered cases of Z. Changes are not significant even if cosφ changes from 0.01 to 0.99 while U_m remains the same. This signifies that the Z of 10 kΩ could be high enough that the working condition under it is considered as a no-load. This is also in good agreement with the waveforms in Figs. 6 and 7.

It has also been found that the value of δI_1 increases with the increase in Z for the same U_m and cosφ. This stands true for most considered cases of U_m. When Z changes from 10 Ω to 10 kΩ, for power factor of 0.99, lowest δI_1 of -0.02% can be found for the case of Z=10 Ω, while the most significant increase in δI_1 has been noted for Z over 100 Ω, reaching up to slightly below 28.5% when transformer is close to no-load working conditions. Similar pattern of change of δI_1 can be noted when considering other power factors. This is most likely due to

the relatively low amplitude of $i_2(t)$ and greater share of magnetising current in the total $i_1(t)$, making the influence of the two approaches more noticeable.

Table 3
Relative differences δI_1 [%] in effective values of primary current between the two considered approaches.

Z [Ω]	U_m [V]			
	30	60	90	120
cosφ=0.99				
0,01	0.22	0.29	0.33	0.34
10	-0.02	0.52	0.6	0.51
10^2	3.31	4.39	3.13	1.29
10^3	21.57	20.48	10.28	1.75
10^4	27.63	26.34	12.23	1.78
10^7	28.42	27.13	12.47	1.78
cosφ=0.9				
10	0.81	1.09	0.88	0.68
10^2	6.79	7.04	4.41	1.82
10^3	22.67	21.54	10.66	1.88
10^4	27.75	26.46	12.27	1.8
cosφ=0.7				
10	1.7	1.67	1.16	0.86
10^2	10.46	9.8	5.66	2.25
10^3	24.29	23.07	11.19	2.02
10^4	27.95	26.66	12.34	1.81
cosφ=0.5				
10	2.6	2.34	1.64	1.25
10^2	13.13	11.77	6.52	2.52
10^3	25.71	24.41	11.64	2.1
10^4	28.14	26.85	12.39	1.82
cosφ=0.3				
10	3.07	2.64	1.94	1.42
10^2	15.52	13.49	7.24	2.73
10^3	27.08	25.71	12.07	2.16
10^4	28.31	27.02	12.45	1.83
cosφ=0.1				
10	3.45	2.85	1.82	1.5
10^2	17.84	15.1	7.89	2.9
10^3	28.45	27.02	12.5	2.21
10^4	28.49	27.20	12.50	1.83
cosφ=0.01				
10	3.6	2.92	1.87	1.53
10^2	18.89	15.81	8.18	2.97
10^3	29.07	27.64	12.69	2.23
10^4	28.56	27.27	12.53	1.83

When comparing the results in **Table 3** for the same Z and U_m, but cosφ changing from 0.99 to 0.01, an increase in δI_1 can be noted for most considered cases, exception mostly being for the cases of 0.01 and 0.1. The reason for such a pattern of change is likely due to the phase-shift in the secondary current, which in cases of low power factor, is almost in-phase with the magnetising current of the core. Therefore, the differences in primary current, found by superposition of the two, are more pronounced than in the other cases. The exceptions observed in some cases of 0.01 and 0.1 power factor are most likely due to the difference in phase-shift of $H(t)$ of hysteresis for different U_m, which can cause the magnetising current to be closer to the phase of $i_2(t)$ for the load power factor of 0.1 than 0.01. This can also explain the reason behind low change in δI_1 for 10 kΩ and 10 MΩ, for different power factors, since secondary current is of too low amplitude for its phase-shift to significantly influence the deference in two approaches (even if its close to being in sync with the core magnetising current). Comparison of $i_1(t)$ for the case of 90 V, 100 Ω and power factor of 0.01, 0.5 and 0.99 is shown in Fig. 12.

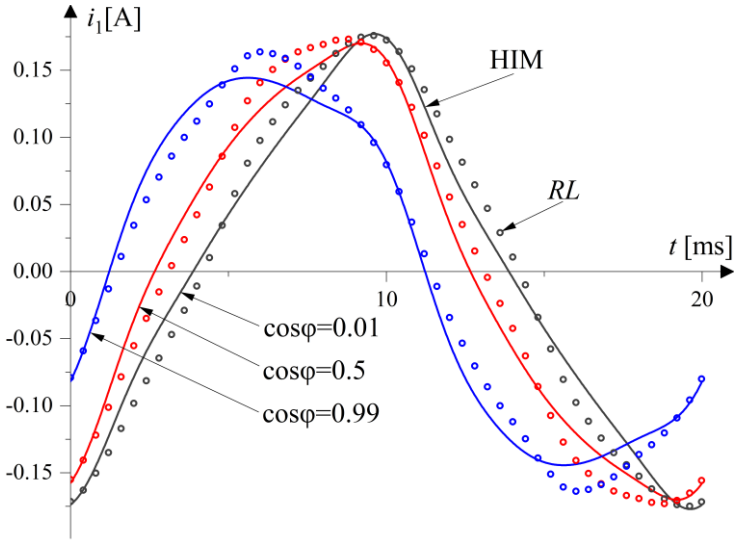


Fig. 12 – *Comparison of $i_1(t)$ obtained using HIM and RL model for Z=100 Ω and cosφ of* 0.01, 0.5 *and* 0.99, *at* 90 V *and* 50 Hz.

The values of δI_1 do not change the same way when comparing the results for the increasing Um while the load remains the same, being lowest for the highest considered U_m. This could be a consequence of used calculation parameters, as R_c has been calculated for the main hysteresis loop while HIM parameters have been found in similar nonlinearity region, which could make both approaches more favorable for calculations in regions with higher

nonlinearity. However, the study necessary to confirm such assumptions is beyond the scope of this paper and will be the subject of future study.

The comparison of the results for $u_s(t)$ for no-load transformer working regime is shown in Fig. 13. The results for $u_s(t)$ for the two considered approaches are in very good agreement for all presented cases. This is mostly due to the low coil resistances in primary and secondary circuits, so the influence of $i_1(t)$ and $i_2(t)$, considered as $R_{N1}i_1(t)$ and $R_{N2}i_2(t)$, is limited. Furthermore, similar behavior regarding the differences in considered approaches has been found for every case of considered load parameters and U_m. Secondary voltage waveform $u_s(t)$ has been calculated using (17):

$$u_s(t) = u_2(t) - R_{N_2} i_2(t). \tag{17}$$

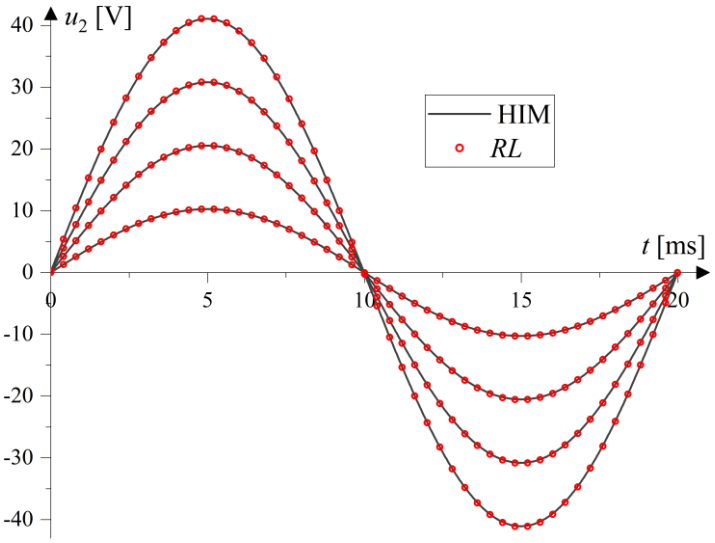


Fig. 13 – *Comparison of $i_1(t)$ obtained using HIM and RL model for Z=10* MΩ *and* $\cos\varphi$=0.99*, Um from* 30 V *to* 120 V *with the step of* 30 V*, at* 50 Hz*.*

Even though the influence of resistances in primary and secondary circuits is low when two approaches are compared on the secondary side, their influence is significant when the amplitude of the voltage is concerned. This is particularly noticeable for lower Z and higher secondary current values. Therefore, the target transformation ratio of 70/24 V/V could not be achieved for the set transformer parameters, if the apparent power of 30 VA were the target. The main reason for this is that the 24 V of the target nominal effective value of $u_s(t)$, U_s, is actually the one corresponding to the ratio of N_1/N_2 for the effective value of $u(t)$, U, of 70 V. This means that the target ratio can only be achieved for the working conditions close to no-load. However, in that case, the current is too low for the

target apparent power. The target apparent power, for the considered transformer parameters, can be achieved for U_s close to 22 V, for both approaches, with *RL* approach yielding slightly lower voltage but higher current than when HIM approach is considered. This means that the real transformation ratio of the transformer in question is 70/22 V/V. The difference between target and realistically achievable U_s is about 9.1% which is lower than the upper limit difference of 10%, commonly considered in practice.

Energy efficiency η is also an important parameter to consider when analysing transformer performance under load. The IEC standard recommends its calculation as the ratio of the apparent output power and apparent output power to which no-load and load losses have been added, for the load power factor of one, at the rated voltage and load [20]. This can be considered as a ratio between output and input apparent power for purely ohmic load. For the simplification purposes in this paper, cosφ of 0.99 has been considered sufficiently high to be considered as very close to purely ohmic. Also, as the load is linear and with such power factor, apparent output power can be considered as mean value of the load instantaneous power. Cooling equipment losses, mentioned in the IEC standard, have been neglected. Based on these assumptions, η can be calculated using (18):

$$\eta[\%] = \frac{\int_0^T u_s(t) i_2(t)\,\mathrm{d}t}{\int_0^T u(t) i_1(t)\,\mathrm{d}t} 100. \tag{18}$$

Calculations have been made for the rated $u(t)$ with the amplitude of 120 V, at industrial frequency of 50 Hz. Load impedance Z has been varied from 0.1 to 200 Ω, with the step of 0.1 Ω, with constant power factor of 0.99. The comparison of η for the two considered approaches is shown in Fig. 14. A very good agreement of the results has been found. This is likely due to the good agreements in $i_1(t)$, as previously showcased and confirmed using **Table 3** results and their analysis, and $i_2(t)$ since the waveforms for $u_2(t)$ are in good agreement. Highest efficiency has been found for 21.2 Ω for both cases, with 84.17% for the iterative procedure and 84.19% for the approach incorporating *RL* model.

However, lowering U_m from 120 V to 60 V, for the same range of Z and the unchanged cosφ, shows significant differences in the efficiency calculations. Comparison of the results for this case is shown in Fig. 15. The results indicate that in the case of the *RL* modeling approach η is higher, which could be of significance when running initial calculations and simulations for the transformer before the beginning of its manufacturing process. In this case, for the first approach, highest η has been found for 83.87% has been found for 20.7 Ω, while for the second its 84.3% at 21.3 Ω.

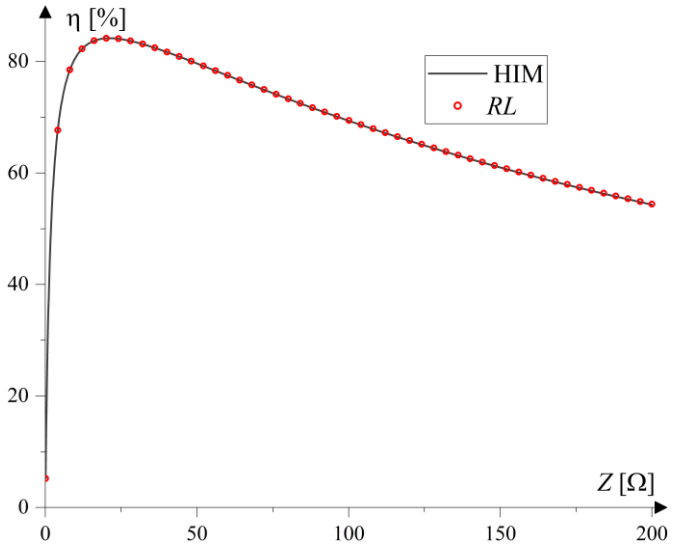


Fig. 14 – *Comparison of η obtained using HIM and RL model for Z from* 0.1 *to* 200 Ω*, with the step of* 0.1 Ω *and cosφ*=0.99*, Um of* 120 V*, at* 50 Hz*.*

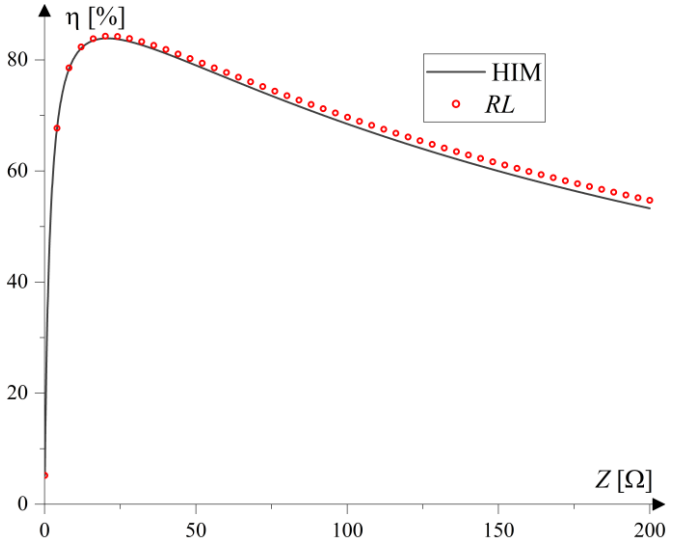


Fig. 15 – *Comparison of η obtained using HIM and RL model for Z from* 0.1 *to* 200 Ω*, with the step of* 0.1 Ω *and cosφ*=0.99*, Um of* 60 V*, at* 50 Hz*.*

The calculations for the achieved transformation ratio of 70/22 V/V and the same power factor of 0.99, reveal the efficiency η of 83.6% for HIM, and 83.7%, for the *RL* approach. The results for η show that the considered transformer is not

very energy efficient, thus not acceptable according to the IEC standard. Increase in η can be managed by changing some of the transformer parameters, such as the thickness of the wire of primary and secondary coils. In this case, the resistance of the coils would be lowered, which in turn would lower the copper power loss. On the other hand, it would also influence the transformation ratio, thus allowing one to achieve the ratio value closer to the target one. The influence of transformer parameter change to the performance of the considered transformer is beyond the scope of this paper and will be the subject of future research.

5 Conclusion

This paper presented an approach to solving an electric circuit with single-phase transformer with ring-shaped core in the time domain. The considered electric circuit consists of AC power supply, single-phase transformer with ring-shaped core, two resistors connected in series with the primary and secondary transformer coils and a load impedance. Calculations have been made for three working regimes of the transformer – no-load, loaded and short-circuit, based on the impedance of the load. Two approaches to time domain calculations have been considered. First approach implemented an iterative procedure based on a combination of HIM and STL methodologies while the second has been a commonly used approach based on transformer equivalent circuit and *RL* model of the core. Parameters for both approaches have been obtained from quasistatic and dynamic measurements. Calculations have been made for sinusoidal input voltage amplitudes from 30 V to 120 V, with the step of 30 V, at the industrial frequency of 50 Hz. Load impedance has been varied from 0.01 Ω to 10 MΩ and its power factor from 0.01 to 0.99.

Based on the results of the previously published research for the circuit very similar to the one considered for no-load conditions, a conclusion can be formulated that the results obtained using iterative procedure are more accurate than those found with the use of *RL* modelling.

Comparing the results of two approaches in the time domain, it has been found that the solutions for primary current waveforms show more significant differences with the increase of the secondary resistance. Also, increasing the load past 10 kΩ has little influence on the waveforms and, as such, can be considered as close to no-load condition for the considered transformer. Similar observations have been made when analysing the relative difference in their effective values. It has been suggested that the reason for that is high amplitude of secondary current, compared to magnetizing one, in the case of lower load resistance, which in turn makes the effects of hysteresis and nonlinearity limited. On the other hand, increase in the amplitude of the input voltage for the same load suggested dependence of difference of the two approaches on the

nonlinearity of the system. This dependence could have a significant influence on the comparison of the approaches and will be the subject of future research. Comparing the results for the same load resistance and voltage, but changing the power factor from 0.99 to 0.01, an increase in effective value differences for the two approaches can be noted for most considered cases. The reason for such a pattern of change is likely due to the phase-shift in the secondary current, which in cases of low power factor, is almost in-phase with the magnetising current of the core.

Differences in transformer energy efficiency are negligibly low for the two approaches when calculated at 120 V. However, for lower voltages the differences increase, especially so when load resistance is high enough for the magnetisation effects to be of higher influence.

When comparing the results for the secondary voltage waveforms it has been found that the two approaches allow for very similar results for the all considered cases.

Fundamental part of the proposed iterative procedure – HIM methodology, is not limited to ring-shaped cores or single-phase transformers. Future research will consider the adaptation of the procedure for the implementation on high-voltage and power, three-phase, and transformers with different core geometries.

6 Acknowledgments

This study was supported by the Ministry of Science, Technological Development and Innovation of the Republic of Serbia, and these results are parts of the Grant No. 451-03-34/2026-03/ 200132 with University of Kragujevac - Faculty of Technical Sciences Čačak.

7 References

[1] B. Koprivica, I. Dimitru, A. Milovanović, O. Caltun: Harmonic Analysis and Modelling of Magnetisation Process in Soft Ferromagnetic Material, Serbian Journal of Electrical Engineering, Vol. 30, No. 1, March 2017, pp. 121 – 136.

[2] G. Shilyashki, H. Pfützner, C. Bengtsson, E. Huber: Time-Averaged and Instantaneous Magnetic Loss Characteristics of Different Products of Electrical Steel for Frequencies of 16 2/3 Hz up to 500 Hz, IET Electric Power Applications, Vol. 16, No. 5, May 2022, pp. 525 – 535.

[3] J. I. Afonso, P. Toscano, I. Briozzo: Current Transformer Modeling for Electromagnetic Transient Simulation in Protection Systems, Proceedings of the IEEE PES Transmission & Distribution Conference and Exhibition - Latin America (T&D LA), Montevideo, Uruguay, September 2020, pp. 1-6.

[4] J. A. Corea-Araujo, J. A. Martinez-Velasco, F. González-Molina, F. J. A. Barrado-Rodrigo, L. Guasch-Pesquer, F. Castro-Aranda: Validation of Single-Phase Transformer Model for Ferroresonance Analysis, Electrical Engineering, Vol. 100, No. 3, September 2018, pp. 1339 – 1349.

[5] Q. Fu, J. Zhu, Z.- H. Mao, G. Zhang, T. Chen: Online Condition Monitoring of Onboard Traction Transformer Core Based on Core-Loss Calculation Model, IEEE Transactions on Industrial Electronics, Vol. 65, No. 4, April 2018, pp. 3499 – 3508.

[6] A. Waindok: A Method for Calculation of the Inrush Current in Single Phase Transformer Including the Residual Flux, Przegląd Elektrotechniczny, Vol. 88, No. 5b, 2012, pp. 194 – 201.

[7] A. Rezaei-Zare, R. Iravani: On the Transformer Core Dynamic Behavior During Electromagnetic Transients, IEEE Transactions on Power Delivery, Vol. 25, No. 3, July 2010, pp. 1606 – 1619.

[8] D. W. P. Thomas, J. Paul, O. Ozgonenel, C. Christopoulos: Time-Domain Simulation of Nonlinear Transformers Displaying Hysteresis, IEEE Transactions on Magnetics, Vol. 42, No. 7, July 2006, pp. 1820 – 1827.

[9] G. Mörée, M. Leijon: Review of Hysteresis Models for Magnetic Materials, Energies, Vol. 16, No. 9, May 2023, p. 3908.

[10] S. Divac, B. Koprivica: Time-Domain Simulation of Electric Circuit with Nonlinear Hysteretic Inductor, Proceedings of the 9th International Conference on Electrical, Electronic and Computing Engineering (IcETRAN), Novi Pazar, Serbia, June 2022, pp. 214 – 219.

[11] S. Divac, B. Koprivica: Solving Dynamic Electric Circuit with Nonlinear Hysteretic Inductor Using Harmonics Interpolation Method, International Journal of Circuit Theory and Applications, Vol. 53, No. 2, February 2025, pp. 545 – 570.

[12] G. Bertotti: Hysteresis in Magnetism – For Physicists, Material Scientists and Engineers, Academic Press, Inc., San Diego, London, New York, 1998.

[13] S. Divac, K. Chwastek, M. Najgebauer, B. Koprivica: Single-Phase Transformer Circuit Solving Using Harmonic Interpolation Method, Proceedings of the 12th International Conference on Electrical, Electronic and Computing Engineering (IcETRAN), Čačak, Serbia, June 2025, pp. 84 – 89.

[14] M. De Wulf, L. Dupré, J. Melkebeek: Quasistatic Measurements for Hysteresis Modeling, Journal of Applied Physics, Vol. 87, No. 9, May 2000, pp. 5239 – 5241.

[15] G. Bertotti: General Properties of Power Losses in Soft Ferromagnetic Materials, IEEE Transactions on Magnetics, Vol. 24, No. 1, January 1988, pp. 621 – 630.

[16] K. L. Kaiser: Electromagnetic Compatibility Handbook, CRC Press, London, New York, 2004.

[17] B. Koprivica, A. Milovanović, M. Đekić: Effects of Wound Toroidal Core Dimensional and Geometrical Parameters on Measured Magnetic Properties of Electrical Steel, Serbian Journal of Electrical Engineering, Vol. 10, No. 3, October 2013, pp. 459 – 471.

[18] S. Divac: A Methodology for Analysis and Solving of Nonlinear Magnetic Problems with Hysteresis in Time Domain, PhD Thesis, Technical Faculty of Čačak, Čačak, Serbia, 2024.

[19] POSCO, Grain Oriented Electrical Steel, 2022, Available at:
http://product.posco.com/homepage/product/eng/jsp/process/s91p2000710e.jsp.

[20] IEC standard - IEC TS 60076-20-2017.